CM-5 | 465

MILITARY TECHNICAL COLLEGE

CAIRO - EGYPT

SIGNAL INTERCEPTION USING CHANNELIZED MICROSCAN RECEIVER

AHMED ELOSMANY*

ABSTRACT

A channelized microscan receiver is used for signal detection and frequency estimation. Its detection performance is theoretically analyzed and is illustrated by presenting its receiver operating characteristics (ROC). The obtained results are compared to that of a wideband radiometer, under the conditions of low input signal-to-noise ratio. The system parameters necessary for frequency estimation within a desired frequency band are determined.

I. INTRODUCTION

Interception of signals is needed for a variety of reasons including reconnaissance, surveillance, position fix, identification, and jamming. For example, an aircraft might attempt to intercept the communications between a submarine or ship and a satellite, or a satellite might attempt to intercept ground-to-ground communications. An interception system basically achieves the three functions of detection, frequency estimation, and direction finding.

There are a number of approaches available for the detection task of signal interception [1]-[6]. One approach employs an *energy detector* or a *wideband radiometer* consisting of a bandpass filter followed by a squaring device and integrator ([1], [5], and [6]). In this approach, the signal is modeled as a stationary Gaussian process with a flat power spectral density. A second approach applies channelized radiometer ([1] and [5]) consisting of a number of branches with each branch measuring energy received in a specified frequency band. This approach has the advantage over the wideband radiometer of providing information on frequency location in addition to making a decision on whether or not signal is present. When desired signals are buried beneath much stronger background noise and interfering signals, conventional radiometry can not perform signal detection and analysis tasks properly [2].

A third approach [3] presents the optimal detection of digitally-modulated signals based on the maximum likelihood criterion. The optimum detector is composed of a bank of receivers which are matched to all possible choices of carrier frequency, phase, and number of symbols and whose outputs are averaged and compared to a threshold. Obviously, this is impossible to implement. A radiometer gives very poor output SNR compared to the optimal detector [3].

In a fourth approach [2], known as *cyclic feature detection*, the signal of interest is modeled as a cyclostationary random process, that is, a random process whose statistical parameters vary periodically with time. The cyclic spectral correlation of the signal is measured and its magnitude is graphed as the height of a surface above a plane with coordinates of frequency f and

* Department of ACG, M.T.C., Cairo

cycle frequency α. This cyclic feature detection technique have the ability to discriminate desired signals against signals not of interest, and reduce sensitivity to unknown and changing background noise level and interference.

A fifth approach [4] presents a compressive receiver as a practical means of implementing a channelized filter bank for signal detection and providing information on frequency location. Its scheme consists of an RF bandpass filter, multiplier with a periodic sweeping waveform followed by a filter, envelope detector, and a sampler. It was shown that the compressive receiver outperforms the wideband radiometer in detecting the presence of a signal.

This paper shows how the tasks of signal detection and frequency estimation are performed using a channelized microscan receiver. The microscan receiver is similar to the scanning superheterodyne receiver [5], except that a chirp filter is used instead of a bandpass filter. In the next section, the channelized microscan receiver is described. Section III presents the derivation of the expressions for the false alarm probability and the detection probability. The corresponding expressions for the wideband radiometer are given in section IV. Section V provides the numerical results of both receivers. Frequency estimation is dealt with in section VI. Conclusions are given in section VII.

II. DESCRIPTION OF CHANNELIZED MICROSCAN RECEIVER

Fig. 1 shows the block diagram of the channelized microscan receiver. The input bandpass filter does not distort the intercepted signal within the scanned frequency range. The input $x(t)$ is described by

$$x(t) = \begin{cases} n(t), & \text{noise alone} \\ s(t) + n(t), & \text{signal plus noise} \end{cases} \qquad (1)$$

where $s(t)$ is the intercepted signal and $n(t)$ is the additive white Gaussian noise of power spectral density η. The scanning generator produces a periodic scanning waveform $y(t)$ which is multiplied by the input $x(t)$ and the product $z(t)$ is applied to $(2N+1)$ chirp filters. Over one scan period T, the signal $s(t)$ and the scanning waveform $y(t)$ are represented, respectively, by

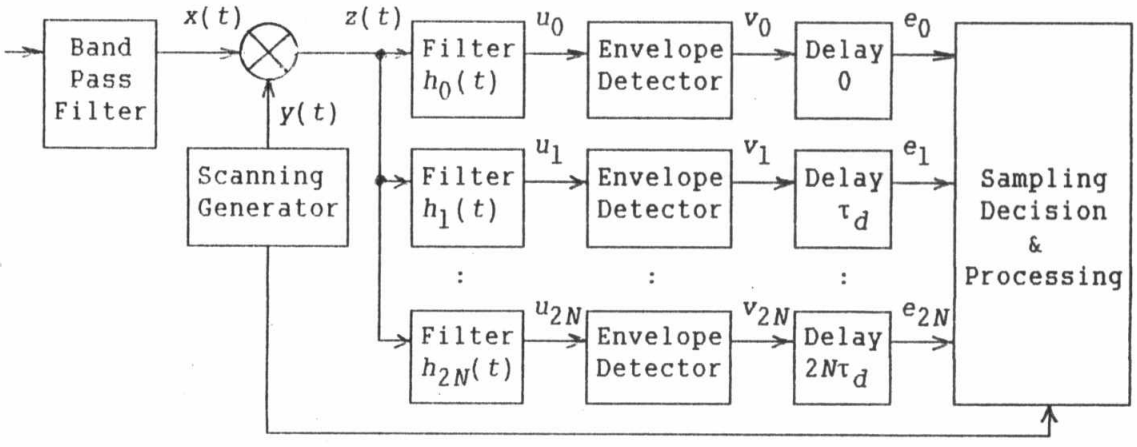

Fig. 1. Channelized microscan receiver

$$s(t) = A \cos (w_0 t + \theta_0), \quad 0 \le t \le T \tag{2}$$

$$y(t) = \cos (w_s t + \pi\mu t^2 + \theta_s) \cdot g_T(t) \tag{3}$$

where $g_T(t) = 1$ for $0 \le t \le T$ and is zero elsewhere. w_s is the angular frequency at $t = 0$, and μ is the scan rate (Hz/second). The impulse response of the i-th chirp filter is described by

$$h_i(t) = \cos (w_{ci} t - \pi\mu t^2) . g_{T1}(t), \quad w_{ci} = w_s - i\,\delta w, \ \{i=0,1,..,2N\} \tag{4}$$

δw ($= 2\pi\delta f$) is the frequency separation between neighboring chirp filters. $g_{T1}(t)$ is a pulse of unit amplitude and duration $T1 \le T$. Input to the chirp filters is given by $z(t) = x(t)y(t)$ and output of the i-th chirp filter is

$$u_i(t) = z(t)*h_i(t) = u_{is}(t) + u_{in}(t) \tag{5}$$

$$u_{is}(t) = [s(t)y(t)]*h_i(t) \text{ and } u_{in}(t) = [n(t)y(t)]*h_i(t) \tag{6}$$

where * denotes convolution. The noise component $u_{in}(t)$ and its statistics are calculated as follows

$$u_{in}(t) = \int_{\tau 1}^{\tau 2} n(t-\tau) \cos[w_s(t-\tau)+\pi\mu(t-\tau)^2+\theta_s] \cos(w_{ci}\tau-\pi\mu\tau^2)\, d\tau \tag{7}$$

where $\tau 1 = \max(0, t-T1)$ and $\tau 2 = \min(t, T)$. For $T1 \le t \le T$ we have $\tau 1 = t - T1$ and $\tau 2 = t$, thus

$$u_{in}(t) \approx 0.5 \int_{t-T1}^{t} n(t-\tau) \cos \phi(t,\tau,i)\, d\tau \tag{8}$$

$$\phi(t,\tau,i) = w_s t + \pi\mu t^2 - 2\pi\mu t\tau + \theta_s - i\delta w\tau \tag{9}$$

The mean value of $u_{in}(t)$ is

$$E\{u_{in}(t)\} = 0.5 \int_{t-T1}^{t} E\{n(t-\tau)\}\cos \phi(t,\tau,i)\, d\tau = 0 \tag{10}$$

The correlation between $u_{in}(t')$ and $u_{jn}(t'')$ is

$$E\{u_{in}(t')u_{jn}(t'')\} =$$

$$= 0.25 \iint E\{n(t'-\tau')n(t''-\tau'')\}\cos \phi(t',\tau',i)\cos \phi(t'',\tau'',j)\, d\tau' d\tau''$$

$$\approx \frac{\eta T1}{16} \frac{\sin(\Omega T1/2)}{(\Omega T1/2)} \cos \left(\frac{\Omega T1}{2} - \Phi\right) \tag{11}$$

$$\Omega = \delta w(i-j) + 2\pi\mu\tau, \quad \Phi = w_s\tau + \pi\mu\tau^2 - j\delta w\tau, \quad \tau = t'-t'' \tag{12}$$

Now consider the following cases. If i = j and $\tau = 0$ then $\Omega = 0$, $\Phi = 0$, and $E\{u_{in}^2(t)\} = \sigma_n^2 = \eta T1/16$ which determines the output noise variance. If i = j and $\tau = m/(\mu T1)$, (m = 1,2,..) then $\Omega T1/2 = m\pi$, and $E\{u_{in}(t)u_{in}(t+\tau)\} = 0$. Thus samples taken from the output of the same chirp filter separated in time by integer multiples of $(1/\mu T1)$ are uncorrelated, hence independent (since they are Gaussian). If $i \neq j$, $\tau = m/(\mu T1)$, (m =0,1,2,..), and $\delta f T1 = 1$ then $\Omega T1/2 = k\pi$,

(k integer) and $E\{u_{in}(t+\tau)u_{jn}(t)\} = 0$. Therefore, samples taken from the output of different chirp filters separated by integer multiples of $(1/\mu T1)$ are uncorrelated, hence independent (if $\delta f T1 = 1$). Clearly, when $\tau=0$ then we have $E\{u_{in}(t)u_{jn}(t)\} = 0$.

The above results indicate that the outputs of different branches of the channelized microscan receiver will be statistically independent if the chirp filter separation δf and the delay τ_d are chosen as follows

$$\delta f = 1/T1 \text{ and } \tau_d = 1/\mu T1 \tag{13}$$

Let us turn to the signal component $u_{is}(t)$. After substitution we get

$$\begin{aligned} u_{is}(t) &= \alpha_{is}(t)\cos(w_{ci}t-\pi\mu t^2) - \beta_{is}(t)\sin(w_{ci}t-\pi\mu t^2) \\ &= R_{is}(t)\cos(w_{ci}t-\pi\mu t^2+\Phi_{is}) \end{aligned} \tag{14}$$

where

$$R_{is}(t)= \sqrt{\alpha_{is}^2(t)+\beta_{is}^2(t)} \text{ and } \Phi_{is}(t)= \arctan[\beta_{is}(t)/\alpha_{is}(t)] \tag{15}$$

$$\alpha_{is}(t) \approx 0.5 \int_{\tau 1}^{\tau 2} s(\tau)\cos(i\delta w\tau+2\pi\mu t\tau+\theta_s)\,d\tau \tag{16}$$

$$\beta_{is}(t) \approx 0.5 \int_{\tau 1}^{\tau 2} s(\tau)\sin(i\delta w\tau+2\pi\mu t\tau+\theta_s)\,d\tau \tag{17}$$

Input to and output from the envelope detector of the i-th branch are given, respectively, by

$$u_i(t) = [R_{is}(t)+\alpha_{in}'(t)]\cos(w_{ci}t-\pi\mu t^2+\Phi_{is}) - \beta_{in}'(t)\sin(w_{ci}t-\pi\mu t^2+\Phi_{is}) \tag{18}$$

$$v_i(t) = \{[R_{is}(t) + \alpha_{in}'(t)]^2 + \beta_{in}'^2(t)\}^{1/2} \tag{19}$$

$v_i(t)$ is then delayed by $i\tau_d$ to give the output of the i-th branch

$$e_i(t)= v_i(t-i\tau_d)= \{[R_{is}(t-i\tau_d)+ \alpha_{in}'(t-i\tau_d)]^2 +\beta_{in}'^2(t-i\tau_d)\}^{1/2} \tag{20}$$

For $T1 \le t \le T$ and when neglecting noise components, then we have

$$e_i(t) = R_{is}(t-i\tau_d) = \frac{AT1}{4}\left|\frac{\sin(w_0-2\pi\mu t)T1/2}{(w_0-2\pi\mu t)T1/2}\right| \tag{21}$$

which at the sampling instant $t_0 = f_0/\mu$ has a peak of $e_i(t_0) = AT1/4$. Since $T1 \le t_0 \le T$, then $T1 \le f_0/\mu \le T$, and $f_{0min} \ge \mu T1$ and $f_{0max} \le \mu T$. The bandwidth (in Hz) to be searched by the receiver is

$$W = f_{0max} - f_{0min} \le \mu(T - T1) \tag{22}$$

Notice that each of the $(2N+1)$ branches has the same peak value, $AT1/4$, at the same sampling instant, f_0/μ.

The $(2N+1)$ output samples are statistically independent, identically distributed with each sample having a Rayleigh density in the noise-alone case, and a Rician density if the signal is present. In the decision, majority-vote rule is applied. Each of the samples $e_i(t_0)$, $\{i = 0,1,..,2N\}$ is

compared with the threshold K. If $N+1$ or more samples are greater than K, then a signal is declared present, otherwise no signal is there.

III. FALSE ALARM PROBABILITY AND DETECTION PROBABILITY

For a single-channel microscan receiver, the false alarm probability is

$$P_{fa} = \text{Prob}\{e_0(t_0) > K \;/\; \text{noise alone}\}$$

$$= \int_K^\infty (r/\sigma_n^2)\, \exp(-r^2/2\sigma_n^2\, dr = \exp(-K^2/2\sigma_n^2) \qquad (23)$$

and the probability of correct decision, that a signal is present, is

$$P_d = \text{Prob}\{e_0(t_0) > K \;/\; \text{signal plus noise}\}$$

$$= \int_K^\infty (r/\sigma_n^2)\, \exp[-(r^2+B^2)/2\sigma_n^2]\; I_0(rB/\sigma_n^2)\, dr = Q(B/\sigma_n, K/\sigma_n) \qquad (24)$$

$I_0(x)$ is the modified Bessel function of the first kind and order zero. B is the value of $e_0(t_0)$ when the noise is neglected. At $t_0 = f_0/\mu$, we have $B = AT1/4$. $Q(a,b)$ is the Marcum Q-function defined by

$$Q(a,b) \equiv \int_b^\infty x\, \exp[-(a^2+x^2)/2]\; I_0(ax)\, dx \qquad (25)$$

For $(2N+1)$-channel receiver, the overall false alarm and detection probabilities are given, respectively, by

$$P_{FA} = \sum_{j=N+1}^{2N+1} \binom{2N+1}{j} P_{fa}^{\,j}\, (1-P_{fa})^{2N+1-j} \qquad (26)$$

$$P_D = \sum_{j=N+1}^{2N+1} \binom{2N+1}{j} P_d^{\,j}\, (1-P_d)^{2N+1-j} \qquad (27)$$

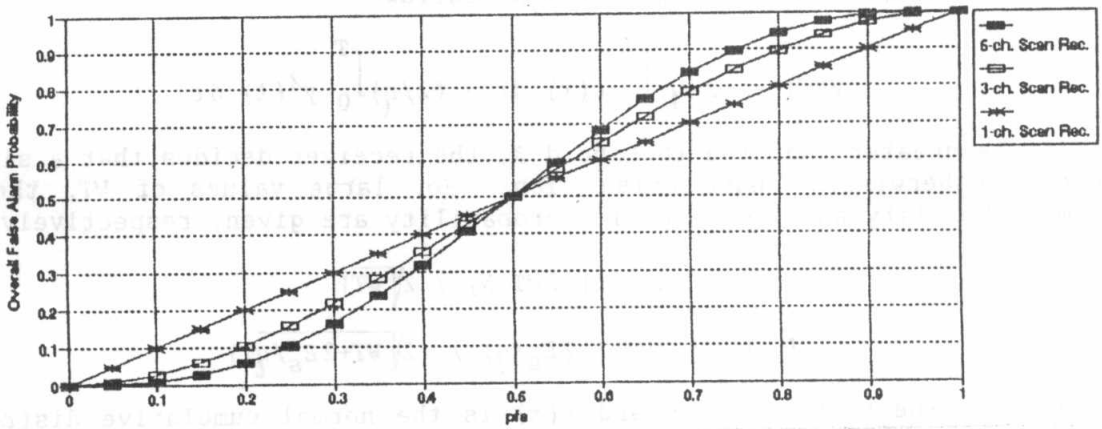

Fig. 2. Overall false alarm probability for channelized microscan receiver.

Notice that the relation between P_{FA} and P_{fa} is identical to the relation between P_D and P_d, thus only one of them is shown in Fig. 2. It is seen that

the multiple-channel receiver gives better performance than the single-channel one, only if $P_{fa} < 0.5$ and $P_d > 0.5$. The improvement gained increases as the number of receiver channel is increased. Solving (23) for K/σ_n and substituting into (24) gives

$$P_d = Q\{\sqrt{\Gamma WTl}\ ,\ \sqrt{-2\ \ln(P_{fa})}\} \tag{28}$$

where Γ is the signal-to-noise ratio given by

$$\Gamma = (A^2/2)\ /\ (\eta W/2) \tag{29}$$

IV. WIDEBAND RADIOMETER

Fig. 3 illustrates the radiometer where the input $x(t)$ may either be the signal plus noise or noise alone. The noise is assumed additive white Gaussian with zero mean and spectral density n. The bandpass filter (BPF) has a center frequency f_0 and bandwidth W wide enough not to distort the input signal. Hence, the output of the BPF, $y(t)$, is

$$y(t) = \begin{cases} n(t), & \text{noise alone} \\ s(t) + n(t), & \text{signal plus noise} \end{cases} \tag{30}$$

where (assuming a pure tone signal)

$$s(t) = A\cos\ (w_0 t + \theta_0) \tag{31}$$

$$n(t) = n_c(t)\cos\ (w_0 t+\theta_0) - n_s(t)\sin\ (w_0 t+\theta_0) \tag{32}$$

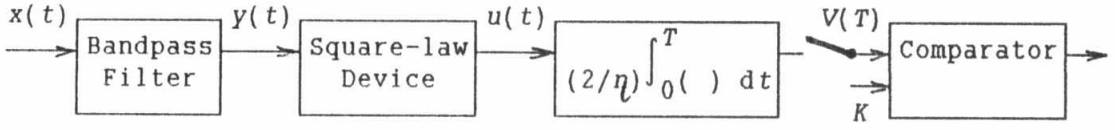

Fig. 3. Block diagram of the radiometer.

The BPF output, $y(t)$, is squared to give $u(t) = y^2(t)$ and then integrated during the interval $(0,T)$ to get $V(T)$ as follows

$$V(T) = (2/\eta)\int_0^T u(t)\ dt = (2/\eta)\int_0^T y^2(t)\ dt \tag{33}$$

If $V(T)$ is greater than the threshold K, the receiver decides that a signal is present, otherwise we have noise alone. For large values of WT, the false alarm probability and the detection probability are given, respectively, by

$$P_{fa} \approx F\{(2WT-K)\ /\ 2\sqrt{WT}\} \tag{34}$$

$$P_d \approx F\{(2WT-K+2E_s/\eta)\ /\ (2\sqrt{WT+2E_s/\eta})\} \tag{35}$$

where E_s is the signal energy and $F(x)$ is the normal cumulative distribution function given, respectively, by

$$E_s = \int_0^T s^2(t)\ dt = A^2T/2 \quad \text{and} \quad F(x) = (1/\sqrt{2\pi})\int_{-\infty}^{x} \exp(-t^2/2)\ dt \tag{36}$$

The derivation of the above formulas can be found in literature (e.g., [1] and [5]). Solving (34) for $(2WT-K)$ and substituting into (35) gives

$$P_d = F\{ [0.5\ \Gamma\sqrt{WT} + F^{-1}(P_{fa})] \ / \ \sqrt{1+\Gamma}\ \} \qquad (37)$$

V. RESULTS

The receiver operating characteristics (ROC) is the plot of the detection probability versus false alarm probability. Figs. 4 and 5 show the ROC of the considered receivers for Γ = -20 dB and Γ = -25 dB, respectively, assuming that WT = 1200 and $T/T1$ = 2. For both types of receivers, as Γ increases, the detection probability P_d increases for the same false alarm probability P_{fa}. The microscan channelized receiver has a better performance than the radiometer, i.e., it has a higher value of P_d for a given value of P_{fa}. As the number of channels increases, performance is improved if P_{fa} <0.5 and P_d >0.5.

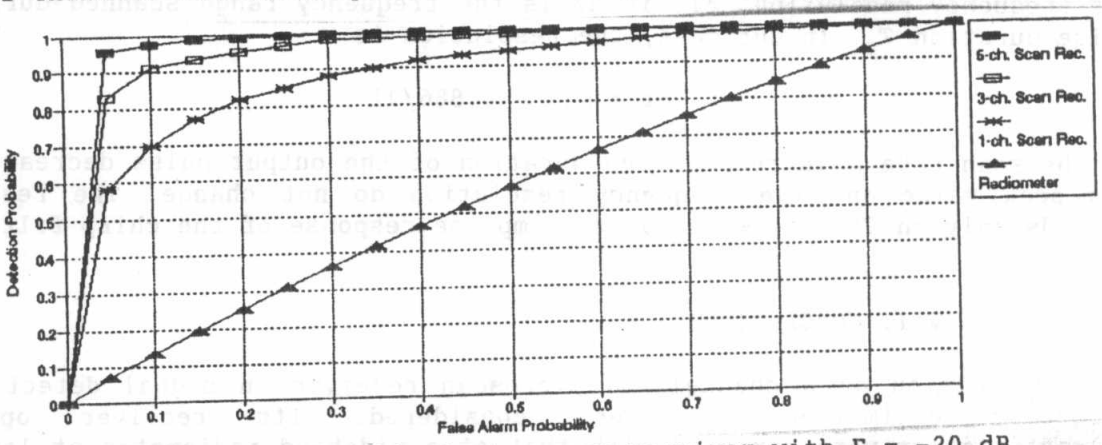

Fig. 4. ROC for the channelized microscan receiver with Γ = -20 dB.

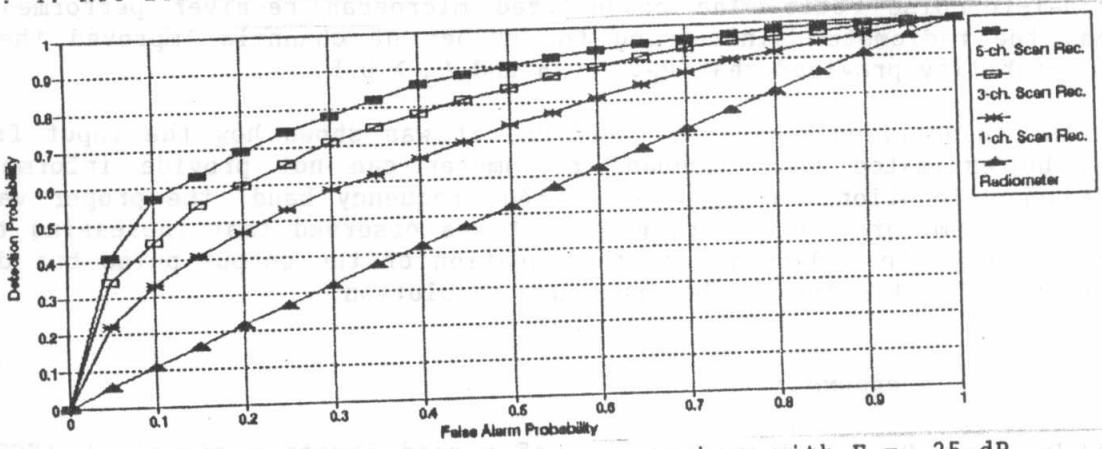

Fig. 5. ROC for the channelized microscan receiver with Γ = -25 dB.

VI. FREQUENCY ESTIMATION

The channelized microscan receiver can be used for frequency estimation as well as for detection. The output of the i-th channel, neglecting noise, is

$$e_i(t) = \frac{AT1}{4}\left|\frac{\sin(w_0-2\pi\mu t)T1/2}{(w_0-2\pi\mu t)T1/2}\right|, \quad T1 \le t \le T \qquad (38)$$

The peak value of $e_i(t)$ is attained at $t_{peak} = f_0/\mu$. Thus, the input frequency f_0 can easily be estimated from the time location of the peak value. This instant lies between $T1$ and T. Therefore, $T1 \leq f_0/\mu \leq T$, i.e., $\mu T1 \leq f_0 \leq \mu T$. The limits of the scanned frequency band are $f_{0min} \geq \mu T1$ and $f_{0max} \leq \mu T$. A proper selection of $T1$ and T is as follows

$$T1 \leq f_{0min}/\mu \quad \text{and} \quad T \geq f_{0max}/\mu \tag{39}$$

$e_{is}(t)$ drops from its peak value , $AT1/4$, to zero as the time t changes from f_0/μ to $f_0/\mu \pm 1/\mu T1$, thus width of the main lobe is $2/\mu T1$. The half-power points of $e_i(t)$ occur at $t_{3dB} = f_0/\mu \pm 0.443/\mu T1$. The pulse duration of $e_i(t)$ between half-power points is found to be

$$T_p = 0.886/\mu T1 \tag{40}$$

The frequency resolution, δf, in Hz is the frequency range scanned during the pulse duration T_p. In our case, the resolution is

$$\delta f = \mu T_p = 0.886/T1 \tag{41}$$

As the scan rate μ increases, the duration of the output pulse decreases, but its peak value and the frequency resolution do not change. The resolution depends only on $T1$, the width of the impulse response of the chirp filter(s).

VII. CONCLUSIONS

The application of a channelized microscan receiver in signal detection and frequency estimation has been considered. Its receiver operating characteristics were compared with that of a wideband radiometer at low input signal-to-noise ratio. The channelized microscan receiver performed better than the radiometer. Increasing the number of channels improved the signal detectability provided that $P_{fa} < 0.5$ and $P_d > 0.5$.

In the channelized microscan receiver, it was shown how the input frequency can be estimated (the wideband radiometer can not provide information on frequency location). To scan a desired frequency band, the proper values of system parameters were determined. It was observed that increasing the scan rate results in a decrease of the duration of the output pulse but does not affect its peak value or the frequency resolution.

REFERENCES

[1] Dillard, R. A., "Detectability of spread spectrum signals," *IEEE Trans. Aerospace Electron. Syst.*,vol. AES-15, pp. 526-537, July 1979

[2] Gardner, W. A., "Signal interception: A unifying theoretical framework for feature detection," *IEEE Trans. Commun.*, vol. 36, pp. 897-906, Aug. 1988.

[3] Krasner, N. F., "Optimal detection of digitally modulated signals," *IEEE Trans. Commun.*, vol. COM-30, pp. 885-895, May 1982.

[4] Li, K. H. and Milstein, L. B., "On the use of a compressive receiver for signal detection," *IEEE Trans. Commun.*, vol. 39, pp. 557-566, Apr. 1991.

[5] Torrieri, D., *Principles of Secure Communication Systems*, Dedham, MA: Artech House, 1985.

[6] Urkowitz, H., "Energy detection of unknown deterministic signals," *Proc. IEEE*, vol. 55, no. 4, pp. 523-531, Apr. 1967.